Non-axisymmetric Hydrodynamic Instability and Subcritical Transition to Turbulence in the Inner Region of Thin Keplerian Discs

Patrick Godon

Jet Propulsion Laboratory
Mail Stop 238-332
California Institute of Technology
4800 Oak Grove Dr.
Pasadena, CA 91109

e-mail: godon@herca.jpl.nasa.gov

September 10, 1997

Abstract

The non-linear growth of non-axisymmetric instability in geometrically thin Keplerian discs is followed numerically with the use of a time dependent two-dimensional polytropic hybrid Fourier-Chebyshev spectral method of collocation. The non-axisymmetric instability (a corotation resonance) develops in tile inner disc when the inner boundary is rigid (corresponding here to the surface of an accreting compact star). All the modes of the instability have a high Q values and a period of rotation of the order of the Keplerian period at the inner edge of the disc. The high order modes have growth rates larger than the low order modes. When the viscosity is large, the higher modes are the first to be damped and saturate at moderate values: the energy is contained in the low order modes which dominate the flow. When the viscosity is low, the high order modes dominate the flow, while the low order modes do not grow: the energy is contained in the higher modes. When the order m and the amplitude a of the unstable mode are high enough (in the present calculations $m \gtrsim 1.5$ and $a \gtrsim 0.3$ for $\alpha = 0.001$), the flow undergoes a subcritical transition to turbulence. The turbulence is confined in the inner region of the disc, inside the 'resonant cavity', where it sustains itself clue to the over reflection of waves (i.e. like the non-axisymmetric instability itself). Some of the low order modes (e.g. m=1 ,5) are dominant during transient phases of the turbulent flow. The turbulence obtained in this work cannot account for angular momentum transport in the disc. However, the instability provides a new robust mechanism to explain the appearance of short period oscillations (Dwarf Nova Oscillations and Quasiperiodic Oscillations) observed in the inner disc of Cataclysmic Variables and other related systems.

Subject Headings: accretion, accretion discs - binaries: general - hydrodynamics - instabilities - stars: oscillations - turbulence

1 Introduction

Papaloizou & Pringle (19S1, 1985, 1987) first demonstrated that a thick disc is unstable to non-axisymmetric perturbations. Additional authors, who also used linear analyses, have given necessary (but not sufficient) conditions for stability (Goldreich & Narayan 1985; Goldreich, Goodman & Narayan 19S6; Goodman, Narayan, & Goldreich 19S?; Narayan, Goldreich & Goodman 1987; Blaes & Glatzel 1986; Glatzel 1987a, 19 87b, 1988, 1989; Sekiya & Shoken 19SS; Jaroszyński 1988; for a review see Narayan & Goodman 1989). Numerical simulations were also used to investigate the non-linear regime of these dynamic instabilities (e.g. Hawley 1987; Blaes & Hawley 19SS; Hawley 1991). A basic amplification process, the over-rdlectioll of waves (Jones 196S; first recognized in discs by Drury 19S0), is responsible for the growth of the instability. A globally unstable mode must have a corotation radius r_c (a radius at which the unperturbed flow rotates with the same speed as the perturbation) within the boundaries of the disc and a reflective radial boundary (Narayan et al. 19S7). When the perturbation, located say at a radius r_p, rotates at a sub-Keplerian velocity $\Omega_p < \Omega_K(r_p)$, its corotation radius is located at a larger radius r_c >7'1,, while when $\Omega_p > \Omega_K(r_p), r_c < r_p$. Assume now a sub-Keplerian perturbation, as it propagates outward the perturbation wave has an angular velocity $\Omega_p < \Omega$ for $r < r_c$, and $\Omega_p > \Omega$ for $r > r_c$, i.e. for $r < r_c$ it has a negative angular momentum (negative action), which changes sign as it crosses the corotation radius. The coronation radius is an evanescent region, into which the wave cannot propagate. '1'here the wave is reflected inward, but in addition it is also partially transmitted outward, due to the tunneling effect. The transmitted wave has a positive angular momentum and consequently, the reflected wave at the corotation radius has more negative angular momentum than tile original incident wave, since the total angular momentum of the wave has to be conserved (Goldreich & Narayan 1985; Narayan et al. 19S7; also known as the wave action conservation, e.g. Lighthill 197S; Spruit 1989). Because of the reflecting inner boundary, tile wave reflected at the corotation radius, will be reflected back toward the corotation radius and thus provides a feedback loop. If an integral number of waves is accomplished within the loop, then the process behaves like an oscillator with a driving force at a resonance frequency ('runaway' oscillator). The same process also occurs for a super-Keplerian perturbation at the outer boundary, if this latter is reflective. If both boundaries are reflective, then the locations of the boundaries will define the relative phases of the inner and outer standing waves. These are also referred to as edge modes, since they grow in the vicinity of the boundaries.

The above theoretical linear analyses and numerical non-linear investigations were carried out for slender and wide annuli/tori. In thick discs and tori systems the non-axisymmetric instability was expected to be strong enough to completely disrupt tile fluid configuration, bringing into question the existence of such systems. However, the lack of a rigid reflective inner boundary in these systems (accretion onto a black hole), made this scenario very unlikely (Blaes 19S7; Hawley 1991; see also Gat & Livio 1992).

In thin Keplerian discs, the rigid surface of the accreting object (say a white dwarf or a neutron star) can provide the reflective inner boundary, however, the growth rate of the modes is smaller (see the linear analysis of Hanawa 198Tb). It was suggested (Narayan & Goodman 19S9) that the unstable modes could provide a viable mechanism to efficiently transport angular momentum, though, numerical simulations (Kaisig 1989a, 1989b) showed that the angular momentum transported in such a case (a local approximation to an inviscid thin Keplerian disc in a Cartesian system of coordinates) is not very efficient. 'l'here was no evidence for the development of turbulence and it has been pointed out (Zahn 1990) that the artificial viscosity might be responsible for the observed saturation of the fluctuations.

A fully two-dimensional numerical analysis of a thin Keplerian disc is still missing, and it the purpose of the present paper to follow the I]oI1-linear growth of a non axisymmetric instability in a fully two-dimensional thin Keplerian viscous disc. Finite-difference numerical simulations are not very well suited to study the instability because higher-order modes have snort radial wavelengths, requiring high spatial resolution, and have low growth rates, requiring integration over many orbits (as already remarked by Narayan & Goodman 1989). Therefore, in this work we use a hybrid Fourier-Chebyshev Spectral Method developed in a previous work to study tidal effects in accretion discs (Godon 1997, Paper 1). Spectral Methods are global and of order $N/2$ in space (where N is the number of grid points). They make use of fast Fourier transforms and are, consequently, relatively fast and accurate when implemented correctly. For this reason Spectral Methods are frequently used to solve turbulent flows (('g. She, Jackson & Orszag 1991; Cho & Polvani 1996a).

In this work, we follow the non-linear growth of non-axisymmetric modes as a function of different physical parameters, mainly the viscosity parameter

α and the disc thickness H/r (or equivalently the inverse Mach number in the disc). In all the cases considered here the unstable modes are located in the very inner part of the disc, adjacent to the inner reflective boundary. When the viscosity is low, the high order modes dominate the flow, while when the viscosity is large, the low order modes dominate the flow. When the order and the amplitude of the unstable mode are high enough, the mode provides the finite amplitude perturbation needed by the flow to undergo a subcritical transition to turbulence. The unstable mode forms inflection points in the inner disc which are unstable and cause the flow to undergo a subcritical transition to turbulence. The turbulence is confined in the inner region of the disc, inside the 'resonant cavity', where it sustains itself due to the over reflection of waves (i.e. like the non-axisymmetric instability itself). Some of the low order modes (e.g. m=5) are dominant during transient phases of the turbulence, but eventually the m=1 mode dominates the flow. Recently, it has been shown analytically and numerically (Balbus, Hawley & Stone 1996, in the context of angular momentum transport in discs) that differential rotation flows (e.g. Keplerian discs), unlike pure shear flows (e.g. Couette Flows), are locally stable to three-dimensional finite-amplitude instabilities. However, this was a local analysis in which it was shown that the initially unstable flow cannot tap energy from the Keplerian flow to grow turbulent. in the present simulations, the instability is global and sustains itself due to the inner reflective boundary. The turbulence taps energy from the flow in the same manner as the non-axisymmetric instability: through the corotation resonance (the over reflection of waves)'. This process cannot account for the angular momentum transport in the disc, since the turbulence is confined in the very inner part of the disc, however, it provides an interesting new mechanism to explain the origin of short period oscillations observed in the inner disc of Cataclysmic Variables and other related systems.

In the next section we present a snort review on the stability of rotating flows which have been related to the study of accretion discs in different contexts. In section 3 we give a snort of outline of the physical assumptions made and the numerical method used to solve the problem. The results are presented and discussed in section 4, where a detailed comparison is made with observations of oscillations in Cataclysmic Variables.

2 Stability of Rotating Flows

It is commonly believed that if an accretion disc can be subject to a hydrodynamic instability that leads to turbulence, then the transition to turbulence will take place only in three dimensions. The justification has been that planar shear flow, which is linearly stable, is unstable to three-dimensional finite-amplitude instabilities (see the review paper of Bayly, Orszag & Herbert 1988). Numerical simulations (Orszag & Kells 1980) have also shown that the transition to turbulence in Couette flow takes place only in three-dimension. And more recently it was realized that the transition to turbulence in three-dimensional (3D) incompressible flow was associated to the presence of streamwise vortices in the flow (e.g. Hamilton & Abernathy 1994). I1OWW'1', a very important detail was omitted: the works of Orszag & Kells (1980) and Bayly et a]. (19SS) were carried out for *incompressible* flow only. 'l'here is no reason to expect the *compressible* flow to behave like the *incompressible* one. In fact two-dimensional (21)) compressible flows are used to represent three-dimensional incompressible flows, since compressibility adds an extra degree of freedom. Therefore, one should be more inclined to think that the 21) compressible flow will behave like the 31) incompressible flow and undergo a transition to turbulence. As an example, the Shalow Water Equations (equivalent to a 2D compressible flow) are used to represent the three-cli]ncnsional incompressible flow in the atmospheric layer. In this section, we review some details of the stability of rotating flows which have been related to the study of accretion discs.

2.1 Stability of Incompressible Couette Flow

In a rotating inviscid incompressible flow, when the equilibrium and the perturbations are axi-symmetric, the specific angular momentum $\ell = r^2\Omega =$ is constant in time, where r is the radius in cylindrical coordi nates (r, ϕ, z) and Ω is the angular velocit y. Such an inviscid incompressible rotating flow is unstable to infinitesimal axisymmetric perturbations when the angular moment um decreases outward $d\ell^2/dr < 0$ (Rayleigh 191 6). The instability leads to the appearance of a secondary stationary flow consisting of the Taylors vortices (there is exchange of stabilities), while the effect of the viscosity is to stabilize the flow below a critical Reynolds number: $Re < Re_c$. Couette flow (i.e. the flow between rotating cylinders), with counterrotating cylinders, is expected to be linearly stable (i.e. stable to infinitesimal perturbations) below a critical Reynolds number, however, the experiments (e.g. Coles 1965; Daviaud, Hegseth & Bergé 1992) have shown that it is subject to a non-linear local instability (i.e. it is unstable to finite amplitude perturbations) that leads to turbulence.

The two different instabilities, linear and non-linear, in the rotating Couette flow lead to two different transitions from laminar to turbulent flow: supercritical and subcritical, respectively. Couette flow with the two cylinders corotating or with the outer cylinder at rest, is linearly unstable according to the Rayleigh criterion and exhibits a supercritical transition to turbulence. The supercritical transition is a progressive and reversible transition to disorder, which takes place as the rotation increases: first the Taylors vortices form and, as the angular velocity increases, a tangential wave pattern appears, and becomes more complicated until the whole flow grows fully turbulent. In this case the turbulent Couette flow is characterized by boundary layers at each cylinders, while the rest of the fluid has a constant angular momentum. Couette flow with counterrotating cylinders, or with the inner cylinder at rest is unstable to finite amplitude perturbations, and shows a subcritical transition to turbulence. This transition is abrupt and localized. The instability is non-linear and leads to turbulent spots in the laminar flow. The flow is divided into regions which are either laminar or turbulent. Waves propagate outwards from the turbulent spots into the laminar regions. As the Reynolds number increases the laminar regions grow scarce until the fluid becomes completely turbulent. Here the turbulent Couette flow is characterized by an enhanced eddy-viscosity proportional to the shear $rd\Omega/dr$ and a Reynolds number $Re \approx 1$.

The subcritical transition to turbulence due to a non-linear instability was followed numerically in three-dimensional incompressible Plane Couette Flow for $Re > 1000$, but was not observed in the two-dimensional case (Orszag & Kens 1980; Dubrulle 1991). The exact amplitude of the perturbations needed for the development of turbulence depends on the Reynolds number (Dubrulle & Nazarenko 1994). The instability coexists with the appearance of inflection points in the mean flow, i.e. local maxima of vorticity in the flow, which are unstable according to the Rayleigh-Fjørtoft criterion (Fjørtoft 1950). The study of the effect of inflection points in an inviscid Couette flow was followed by Lerner & Knobloch (1988), and Dubrulle & Zahn (1991) extended the case to a viscous flow. It has been shown more recently that the existence of streamwise vortices is involved in the destabilization process that leads to turbulence in the three dimensional incompressible flow (e.g. Hamilton & Abernathy 1994; Dauchot & Daviaud 1994, 1995a, 1995b; Hegseth 1996). A streamwise vortex induces an inflection point in the flow, which is unstable. This process is purely three dimensional, and cannot take place in two dimensions, which explains the results of Orszag & Kell (19S0) and Dubrulle (1991). The streamwise vortices tap energy from the rotating flow, and then pour it into the turbulence. If this mechanism was to work in a 3D disc, the vortices would be oriented in the angular direction (Dubrulle 1997). However, it has *not* been shown that the same three-dimensional mechanism (i.e. the streamwise vortices) is responsible for the destabilization of compressible rotating flows.

2.2 Stability of Compressible Couette Flow

It is not clear how compressibility will affect the flow, since it adds an extra degree of freedo1"1 . It is important to stress that only a few studies have been carried out for supersonic rotating flows, where compressibility starts to affect the flow. In the limit of small values of the Mach number, the dominant instability is of the Kelvin-Helmotz type, while for large values of the Mach number the instability is the (two-dimensional) centrifugal instability (e.g. Tomasini, Dolez & Léorat 1 996). In their work on transonic shear flows, Tomasini et al. (1996) did not rule out turbulence, though it was not obtained numerically.

2.3 Stability of Atmospheric Flow

'l'he atmospheric ffow is presented here as an example of a linearly unstable 2D compressible flow. Two-dimensional models of the atmospheric shear flow on a rotating surface have a lot of similarities with the two-dimensional Keplerian flow (differential rotation, Coriolis force; see e.g. Cho & Polvani 1996a, 1996 b). The atmospheric flow is really a three dimensional incompressible flow, however it is represented by the shallow-water equations (SWE), which are completely equivalent to the equations of a 2D compressible flow. Two-dimensional inviscid Keplerian discs can be represented by the SWE, where the depth h of the shallow' water flow is proportional to the surface density of the disc Σ (and therefore there might be some links between the behaviour of the two different flows). In the SWE the shear flow is unstable to waves longer than a critical value. These waves have a phase speed that mat ("1)('s the mean current velocity within the flow, which permits a transfer of energy from the current to the wave. This process is known in geophysical fluid dynamics as *barotropic instability* (Pedlosky 1987; Cushman-Roisin 199 4).

This instability is linear and is I)cli('vet] to be responsible for the formation of turbulence in the atmosphere on the large two-dimensional scales which transport angular momentum (the small scales are not affected by the rotation and can be represented by three dimensional homogeneous turbulence with a Kolmogorov energy spectrum).

It is interesting to remark that while the 21) geophysical flow (represented by the shallow water equations) is unstable to the Coriolis forces, 2D transonic shear flows (like the one studied by Tomasini et al. 1996) arc unstable to centrifugal forces. In discs, both the centrifugal and the Coriolis terms are present, however the centrifugal force is balanced by the force of gravity.

2.4 Stability of Differentially Rotating Discs

Rayleigh (1916) has shown that a rotating flow is stable to infinitesimal non-axisymmetric perturbations when there is no local extremum in the vorticity. However, compressibility adds an extra degree of freedom, which allows the appearance of linear non-axisymmetric unstable modes in the case where the angular velocity is a power law of the radius (Goldreich & Lynden-Bell 1965; Stewart 1975, 1976). Compressibility becomes important when the flow velocity becomes supersonic and shocks start to form. In accretion discs the rotation speed is supersonic, $\Omega \propto r^{-p}$ and the vorticity is monotonous w $= |\nabla \times \vec{v}| \propto (2 - p)\Omega$ (with $1 \leq p \leq 2$). If a small non-axisymmetric perturbation (say δP) is introduced, then the angular momentum equation gives:

$$\frac{d\ell}{dt} = -\frac{1}{\rho}\frac{\partial \delta P}{\partial \phi}, \tag{1}$$

and the specific angular momentum is no longer constant (where p is the density). In this case $d\ell^2/dr < 0$ for some range of r within the boundaries ensures instability, however, $d\ell^2/dr > 0$ for all r within the boundaries does not especially exclude instability (Chandrasekhar 1961). The most general and sufficient stability condition for non-axisymmetric perturbations is that of a rigid rotation, i.e. Ω constant (e.g. Sung 1974; Hanawa 1986, 1987a; Fujimoto 19 S7').

3 Numerical Modeling

All the details on the numerical method and the exact form of the equations can be found in Paper I, therefore, we give here only a short outline of the numerical modeling.

3.1 Physical assumptions

The full Navier-Stokes equations are written in cylindrical coordinates (?", ϕ, z), and are solved in the plane of the disc (r, ϕ). We use an alpha viscosity prescription for the viscosity law, and assume a polytropic equation of state. We chose n = 3 for the polytropic index and the polytropic constant is fixed by chosing H/r at the outer radial boundary R_{out}, i.e. by chosing the 'temperature' of the disc. A cold disc has $H/r \approx$ a few percent, while for the hot disc case $H/r \approx$ 0.1 -- 0.2. Unless otherwise specified, in the models presented here, the outer radius of the computational domain is located at $R_{out} = 5R_{in}$, where R_{in} is the inner radius of the computational domain.

3.2 Boundary and initial conditions

The outer radial boundary is a free boundary, i.e. it is treated with non-reflective boundary conditions. At this boundary ρ, v_r and Ω are given, e.g. the solution of a standard thin Keplerian disc.

The inner boundary is treated as a rigid fast rotating accreting object. At the present stage of the work we ignore the boundary layer between the disc and the star. However, the sharp density drop in the boundary layer seems to reflect waves very efficiently (Godon 1995). This makes our present reflective inner boundary assumption valid for a wider range of problems including the one Of the boundary layer. Consequently, we chose $v_r =$ O, $\Omega = \Omega_K$ and ρ is not given, since this would overspecify the boundary conditions. (see paper 1 for all the details of the treatment of the boundary conditions)

The initial density is uniform, the initial rotation law is Keplerian and the radial velocity is initially set to zero. The equations are first solved in one dimension, and after an initial dynamical phase of relaxation, the equations are solved in two dimensions. The initial infinitesimal perturbation of the disc is either provided by the tidal potential of a companion of very small mass (like in Paper 1), or by a random 'noise' in the density. The results obtained using the two different initial perturbations are the same. In most of the cases, we decided to use a very weak perturbating tidal potential to provide the initial non-axisymmetric perturbation. This has the advantage of being a 'natural' way to disturb the system.

3.3 The numerical scheme

In order to follow the non-linear growth of the instability, we use the time dependent hybrid Fourier-Chebyshev method of collocation developed in Paper 1. A Chebyshev expansion is carried out in the radial direction, while a Fourier expansion is used in the angular direction. We solve the time dependence of the equations by means of an explicit 4th order Runge-Kutta temporal scheme. We take 64 points in the radial dimension and 32 points in the angular dimension (64X32) for models with a moderate viscosity ($\alpha \approx 0.1$). For models with a lower viscosity ($\alpha \approx 10^{-3}$) we take higher resolutions: $256X32$, $256X64$ and $128X128$. When the viscosity ν is constant, one can solve the viscous term implicitly in a very efficient manner, by writing the equations in the spectral space. One is then left with a diagonal banded matrix, easy to inverse (see e.g. Canuto et al. 1989; this was applied by Tomasini et al. 1996). However, in the present case the coefficient of the viscosity ν is not constant, ($\nu = \alpha c_s H$). Consequently, the time dependence of the equations is solved using an explicit fourth-order Runge-Kutta method, and the Chebyshev method is implemented using the modification described by Kosloff & Tal-Ezer (1993). This allows one to run the code efficiently on a work station.

In the radial direction we use a spectral filter to cut-off high frequencies. This implementation is used for numerical convenience. It gets rid of the high frequencies which can cause numerical instability, while it keeps a high enough number of terms in the spectral expansion to resolve the fine structure of the flow (see e.g. Paper 1, but also Gottlieb & Orszag 1977; Voigt, Gottlieb & Hussaini 1984; Canuto et al. 1988; a specific application can be found in Don & Gottlieb 1990). The models with a low viscosity ($\alpha \approx 0.001$) are unstable to high order modes of the Papaloizou-Pringle instability. The order of unstable modes reaches a very high value. In order to follow the evolution of the Papaloizou-Pringle instability in the low viscosity models one has to make sure that the highest unstable modes are not the highest mode of the resolution. This means that one can either increase the resolution or damp the higher modes of the resolution. In the present simulations we damp the higher modes by using a spectral filter in the angular dimension. The filter we use has the same analytical form as the filter used in the radial direction, it cuts-off exponentially the high frequencies above a given frequency k_0 (see paper I for details). It, acts like a an artificial viscosity on the mode $k > k_0$.

This filter is also necessary in order to follow the turbulence: it is here similar to the strong cutt-off of the high frequencies obtained with a high power (p) of the dissipation operator used in the numerical study of turbulence (e.g. Cho & Polvani 1996a). It does not affect the transition to turbulence or the turbulence itself, but only the detailed structure of the flow. The high power dissipation) operator permits to extend the inertial range of the turbulence to higher frequencies (k).

4 Results and Discussions

We have run models with different values of the physical and numerical parameters. We have varied the viscosity parameter α, the Mach number in the disc $M = v_K/c_s$, the resolution and the spectral filter. Not all the models are presented here.

4.1 Preliminary considerations

4.1.1 Conditions for instability

We found that the non-axisymmetric instability does not develop for $\alpha > 0.04$ and M < 14, which means for a high viscosity, since $\nu = \alpha c_s^2 \Omega_K^{-1}$ (i.e. models with $M < 14$ require $\alpha < 0.04$ to become unstable, while models with $\alpha > 0.04$ require M > 14). This is justified by the fact that the viscosity damps the waves which are responsible for the growth of the instability. In addition, as expected, the non-axisymmetric instability develops when the inner boundary is reflective. In all the models presented here, the inner boundary is rotating at the Keplerian velocity, i.e. we ignore the boundary layer (In order to take into account the boundary layer between the slowly rotating stellar surface and the Keplerian disc, we would have to increase the resolution by a large factor). However, in the boundary layer there is a sharp transition where the flow becomes sub-Keplerian and is partially sustained by the pressure. There the density drops by several orders of magnitude. This abrupt change in the density is prone to reflect, incoming waves: the waves will not propagate into the low density (sub-Keplerian) region. And it is therefore a good assumption to assume that the reflective boundary is the high density region where the rotation is still Keplerian (we also discuss the issue of the boundary layer in the conclusions section). On the other side, some systems might have a fast rotating accreting star. It is enough for a white dwarf (in Cataclysmic Variable systems) to accrete $\approx 0.1 - 0.15 M_{\odot}$ to rotate near break up (Narayan & Popham 1989) and at this stage it can still continue to accrete (Popham & Narayan 1991). In addition, many CV systems do not show observational evidence of a boundary layer (Ferland et a l 1982). In these systems, it could well be that only the outer envelop of the star is rotating near break up.

4.1 .2 Growth rate of the unstable mode

111 all the models we found that the growth rate ω_i of an unstable mode (m=i) varies between ω_i/Ω_K 2310-3 – 10-2 in agreement with the results of linear studies for thin Keplerian discs (Hanawa 1987b; Kaisig 1989; Savonije & Heemskerk 1 990). This means that one has to follow the simulations over a time scale of the order of at least $\approx$ 100 – 1000 local orbits at the inner edge of the! disc, in order to discern the unstable mode in the density profile. in contrast, in the thick discs case the instability needs to be followed only over a few orbits (Papaloizou & Pringle 1984; Hawley 1987). In Paper 1, some models were followed over a time scale $\approx$ 10'1 periods, while here most of the models arc followed 011 a period of the order of $\approx 10^3$ local orbits. The growth rate of a particular mode increases with increasing viscosity (e.g. see Table 1). This can be explain simply because the higher the viscosity, the shorter the accretion time needed to accumulate (non-axisymmetric) matter in the inner disc.

4.1.3 Effect of the viscosity

The high order modes have growth rates larger than the low order modes. Consequently, when the viscosity is low, the high order modes dominate the flow, while the low order modes do not grow (the energy is contained in the higher modes). When the viscosity is large, the higher modes are the first to be damped and saturate at moderate values, the energy is then contained in the low order modes which eventually dominate the flow (see also Table 2).

Models with a low Mach number ($M \approx 5 - 10$, hot discs) were run with $\alpha = 0.01$ (and a resolution of 64X32). Initially, the m=4 mode is dominant but after a few dozen of orbits the dominant mode is the m=2 mode (e.g. model 3 in Paper I). Models with a high Mach number ($M \approx 20 - 60$ cool discs), run with $\alpha = 0.1$ (and a resolution 64X32), showed that the dominant mode is of order m=2 (like in models 1 and 2 in Paper I). When the viscosity is decreased to α = 0.01 (with a resolution of 256X32) the m=8 mode is initially the dominant one, but eventually the order of the mode changes to m=7,6 and eventually the dominant mode becomes the m=5 mode (this is the case for model 5 in Paper 1, which was run further in the present work). We have also run cool discs with α = 0.001 (and with resolutions 256X64 and 128X128) and found that the dominant mode was very high (m > 15). These low viscosity models were run with a spectral filter in the angular direction (see the section on the numerical method). The effect of the viscosity on the order of the dominant mode is recapitulated in Table 3.

4.2 High viscosity and low order modes.

We have carried out a systematic study of an m=2 mode in a cool disc as a function of the viscosity. The m=2 mode is dominant in a cool disc when $\alpha \approx$ 0.1. It forms a precessing elliptic density pattern around the central object, with a period close to the Keplerian period in the inner disc. The mode has a very coherent period and phase. This suggests that the unstable mode could be the source of short period coherent oscillations observed during outburst of Cataclysmic Variables (discs around non-magnetic White Dwarfs, e.g. Patterson 1981 ; Warner 1986; for some recent results see Mauche 1996) and maybe around Neutron Stars in Low-Mass X-ray Binaries (e.g. Mason et al. 1980; Sadeh et al. 1982; Schoelkopf & Kelley 1991; or more recently Strohmayer et al. 1996). An additional tests, that we carried out to verify this suggestion, was to check how the period of the unstable mode varies as a function of the Luminosity of the disc, i.e. as a function of the mass accretion rate. The solution of the polytropic disc is independent of the value of the density. Consequently, we assume that the mass accretion rate is proportional to the viscosity parameter α. The effects of the viscosity on the m=2 mode is shown in table 1. For $\alpha \approx$ 0.1, we find that the period of the mode P varies with the mass accretion rate $\dot{M}$ as $P \propto \dot{M}^{-\beta}$, where $\beta \approx 0.1$ in good agreement with the slope of the original 'banana diagram' ($\beta \approx$ 0.2, Patterson 1981), and the more recent observations of SS Cyg ($\beta \approx$ 0.1, Mauche & Robinson 1997). In this latter system the observed jump of the oscillations from a period of $\approx$ 6s to $\approx$ 3s (Mauche & Robinson 1997; van Teeseling 1997) can be easily interpreted as a change of mode from m=1 to m=2. In the next section we propose an additional explanation to the "jump" of the mode observed in SS Cyg.

4.3 Low viscosity, High order modes, and transition to turbulence

When the viscosity is further reduced in the cold disc, $\alpha \approx$ 0.001, the higher modes (m > 15) are dominant and sat urate at a much higher value than when $\alpha \approx$ 0.1. The modes rather look like 'planets' (i.e. high density islands, like in the results of Hawley 1987), inducing waves that propagate outwards. Figure 1 shows such a result for a model in which the m= 16 mode is dominant. in this model the resolution is 256X64 and a spectral filter is applied in the azimuthal direction, With a cutoff frequency of k_0 = 16. The frequencies above k_0 are clamped by the filter, and therefor the m==16 mode is the dominant one. It saturates with an amplitude of $\approx$ 0.1. The inner disc stays in this state for more 500 local orbits after the mode has grown unstable, time at which we arbitrary decided to stop the simulations.

4.3.1 Non-1 inear evolution of a turbulent model

We carried out several additional test models (not all shown here) and found out that when the order m and the amplitude a of the unstable mode are high enough (in the present calculations $m \gtrsim$ 15 and $a \gtrsim 0.3$ is obtained by chosing α = 0.001), the mode provides the finite amplitude perturbation needed by the flow to undergo a subcritical transition to turbulence. in figure 2 we show the appearance of an m=19 unstable mode in the inner disc (in model 2 k_0 = 20). After the mode has grown exponentially, it seems to saturate with an amplitude of $\approx$ 0.3. A closer look at the amplitude of the mode reveals that the mode still grows linearly at a very low rate. At a time of $t \approx 650$ all the modes (with $k < k_0$) start to growth and the flow becomes turbulent (see also figure 7). The turbulence is confined in the inner region of the disc, from which waves propagate outward (figure 3. though very different in nature, the present turbulence has the same appearence as turbulent spots with outward propagating waves; e.g. Dauchot & Daviaud 1994, 1995a & b). Some of the low order modes (m=5) are dominant during transient phases of the turbulent flow. But eventually the m= 1 mode becomes dominant and remains so for the rest of the run (for about 300 orbits).

The velocity fluctuations of the turbulence are subsonic (with a Mach number M=0.5-0.7). By the end of the run (around t=1200) small Shocks start to form and the fluctuat ions become supersonic. '1'11(' 1110(1 ('[was stopped at this stage, since the spect ral methods cannot resolve resolve shocks (d ue to the Gibbs phenomenon). Other models have developed supersonic fluctuations at an earlier stage of the evolution and the turbulence could be followed for only 50 orbits, while in the present model the turbulence was followed for over 500 orbits (from $t \approx 700$ to $t \approx 1200$). The total kinetic energy of the fluctuations is shown in figure 4. At the early stage of the evolution ($t < 300$) there is only small fluctuations ('noise') due probably to the initial relaxation of the model and small amplitude viscous oscillations in the disc (see also Paper 1). As the $m=19$ mode continues to grow, the kinetic energy contained in it eventually becomes larger than the 'noise' and the exponential growth of the energy becomes evident ($300 < t < 400$). The saturation of the mode is seen clearly for $400 < t < 600$. Then around $t \approx 650$ the flow becomes turbulent and the kinetic energy grows again, but it also oscillates with a large amplitude (it is interesting to compare figure 4 with figure 7). The fast and oscillatory growth of the kinetic energy around t=700 is associated with and characteristic of the higher m=19 mode. The energy then decreases while the dominant mode changes from m=19 to m=5 and eventually m=1 (around t=900). At this stage the kinetic energy starts to grow again, more slowly and also more steadily, characteristic of the low order m=1 mode. A look at the power spectrum of the energy reveals immediately the dominant modes m=1,5, and 19 (figure 6).

4.3.2 The Power Spectrum

The power spectrum of the kinetic energy integrated over the turbulent region and in time is shown in figure 6 (in figure 5 the same is shown before the transition to turbulence, while the m=19 mode is dominant). The Fourier transform of the kinetic energy has been carried out only in the angular direction, since in the radial direction the turbulence covers only a small region (and therefore only ≈15 grid points). The slope of the spectrum is roughly -1 (though at some stage of the evolution the slope is closer to -1.5). At this stage of the work it is difficult to assess how accurate is this value of slope. One might need to increase the number of points in the angular direction from M=64 to M= 128, 256 or even 512 in order to be confident with this result.

The only other turbulent flow with which we can compare our results is the rotating two-dimensional model of the atmosphere (using the shallow water equations, Cho & Polvani 1996a). As stated in the second section this flow is equivalent to a 2D compressible rotating flow. There the index of the slope varies between ≈ -3 and ≈ -4 and depends somewhat 011 the initial conditions and on the dissipation parameter p. However, as has been pointed out (Cho & Polvani 1996a) many spectral behaviours are possible, and comparisons of spectral slopes (with spherical or planar results) should not be tempted.

'I'he only comparison which can be made is the following. In the three-dimensional incompressible turbulent atmosphere of a rotating planet the larger scales are affected by the Coriolis form and probably also by the finite vertical extent of the atmospheric layer. The deviation from a Kolmogorov spectrum is strong and the energy spectru m behaves like $E_k \propto k^{-3}$ (e.g. Dubrulle & Valdettaro 1992). The large scales are most probably two-dimensional in structure. The smaller scales are not affected by the rotation (the Eddy turn over time is much smaller than the rotation time) neither by the small vertical extent of the at mospheric layer. Therefore, on this scale, the turbulence remain homogeneous, thre-dimensional and the Kol mogorov inertial range still holds there $E_k \propto k^{-5/3}$.The same is probably true also in discs, and one might expect the large scale turbulence ($\lambda > H$) to be affected by the rotation and the the small thickness of the disc. One can therefore say that the large scale turbulence which transports angular momentum will be two-dimensional and non-homogeneous, while the small scale turbulence ($\lambda < H$) will be three-dimer isional and homogeneous (with a Kolmogorov spectrum).

4.3.3 The energetic

The non-axisymmetric instability grows according to the mechanism describe in the introduction: it grows due to the over-reflection of waves, while it is confined in the resonant cavity. This mechanism transfers, through waves, ene rgy to the unstable modes. The instability produces inflection points in the flow which, at some stage (when the perturbation is strong enough) makes the flow unstable and turbulent. '1111(' turbulence thin, in order to sustain it-self, taps its energy from the flow in the same manner as the instability itself: through the over reflection of waves. In fact one can look at the tu rbulen ce as a non-axisymmetric instability where all the n nodes have grown unstable. The turbulent pattern rotates at the same speed as the init ial non-axisymmetric instability, from which it formed. It has the same a corotation radius. This explains why the turbulence is co n fined only in the resonant cavity, between the corotation radius and the inner edge of the disc. There is no amplification of the short waves propagating outwards (from the resonant cavity), since there is probably still too much viscosity for waves of that amplitude (the viscosity increases with radius and the resolution decreases with radius).

4.3.4 Comparison with Observations

In order to make further comparisons with the observations, we assume (as a first approximation) that the luminosity of the inner disc is proportional to the energy dissipated them (our model is poylitropic). We compute the dissipation function $\Phi(t)$ as a function of time for two different cases: first for a whole ring with $0 \leq \phi \leq 2\pi$ (say $\Phi_{2\pi}$) and then for half a ring with $0 \leq \phi \leq \pi$ (Φ_π). The first case enables to discern intrinsic change in the dissipation function as a function of time. The second case reproduces the eclipse of the inner disc by the central star, but enables also to discern non-axisymmetric rotating (luminosity) pattern. 111 figure s we show $\Phi(t)$ for the two cases around i $\approx$ 770, just after the flow became turbulent. This is a transient phase in which the dominant mode changes from m=1 9 to m=5 and eventually to m=]. The inner disc reveals an intrinsic change in Φ (obvious when looking at $\Phi_{2\pi}$) of large amplitude ($\approx$ 10 percent) with a frequency $\nu = 2\nu_0$, where ν_0 is the freq uency of the rotating fluctuations (slightly smaller than the local Keplerian frequency ν_K, since the coronation radi us is larger than the inner radi us of the disc). The variation of $\Phi_{2\pi}$ is very much sinusoidal and highly coherent. This variation is probably associated with the forward and backward travel of waves in the resonant cavity, which is the process that sustains the instability and the turbulence. A look at Φ_π, however, shows a variation much less sinusoidal and less coherent. Some additional frequencies can be discerned, like $\nu = \nu_0$, $\nu = 3\nu_0$ and $\nu = 5\nu_0$. These are the odd dominant modes 111=1 ,3 and 5. The even modes can not be seen since they cancel themselves while rotating (as a fluctuation disappears behind one side of star, another one reappears 011 the other side). The $\nu = 2\nu_0$ frequency is also apparent (due to the intrinsic change in Φ).

A look at the same graph but around $t \approx 1100$ (figure 9) shows a completely different picture. At this stage the m=1 mode is dominant. The inner disc stays in this stage for about ≈ 300 local Keplerian periods until the simulation is stopped. The quantity $\Phi_{2\pi}$ reveals two periods of intrinsic changes (and of small amplitude): $\nu = 2\nu_0$ (the same as previously, but its amplitude has decreased) and $\nu \approx 0.08\nu_0$ (corresponding 10 a period f' = 12.4 Iota] Keplerian periods). This low frequency oscillation is transient and is associated with the eccentric oscillations of the whole disc as the one observed in the run of model 5 in Paper I (but not mentioned there; this kind of oscillations was also observed in the results of Różyczka & Spruit 1993). In the inner disc, however, the rotating dominant m=1 mode produces a highly sinusoidal and coherent oscillation with a frequency $\nu = \nu_0$, which is observed in the graph of Φ_π in figure 9. In contrast to the case in figure 8, the rotating m=1 mode in the inner disc can illuminate the whole disc, such that an observation of the reprocessed light will in fact reveals the frequency $\nu = \nu_0$ (this is difficult to reproduce if several modes are dominant, like in figure S for Φ_r around $t \approx 770$ with the frequencies $3\nu_0$ and $5\nu_0$).

'1'0 summarize and compare, we have distinguished three kind of oscillations related to the turbulent inner disc. The first with a frequency $\nu = 2\nu_0$ is due to an intrinsic change in the luminosity of the disc and is mainly seen during a transient phase of the turbulence, while the energy is in the higher modes (after what the amplitude Of this frequency decreases). The second oscillations with a frequency ν_0 can be observed directly due to the occultation of the inner disc by the central star or indirectly if its light is reprocessed by the whole disc. This oscillations is due to an m=1 rotating mode and is seem after the initial 'relaxation' phase of the turbulence, when the energy is passed to the m= 1 mode.

We propose that these two oscillations, which are highly coherent and sinusoidal, are the oscillations which are usually observed as Dwarf Nova Oscillations (DNOs) in Cataclysmic Variables. The m= 1 is the fundamental mode of the oscillation] and is it the one which is usually recognized as the DNO: its m=1 symmetry allows for the 360 degree shift in the phase when the source is eclipsed by a companion star (with a jump of 180 degree at Inicl-eclipse; Patterson 1981). While the $\nu = 2\nu_0$ oscillations is probably observed as its first harmonic (first harmonics have been observed in AE Aqr by Patterson 1979) or during a transient phase of the disc (e.g. at maximum light during outburst; Mauche & Robbinson 1997). It would be interesting to check if the first harmonic observed in SS Cyg (or AE Aqr) also undergoes a phase shift of 360 degree during eclipse. We postulate that if it is due to the process described here, the first harmonic will not undergo any phase shift during eclipses from the secondary. If it is due to a splitting of the mode from m= 1 to m=2 (as proposed in the preceding subsection), then it will exhibit a phase shift of 180 degree (with no phase jump during mid-eclipse). It has been proposed long ago (Bath 1973) that the DNOs are due to eclipses of transient hot spots at the inner edge of the disc. Models of boundary layers (e.g. Kley 1991; Godon 1995; Hujeirat 1995) have not been able to provide oscillations highly sinusoidal *and* with Keplerian periods. Here we propose a 'robust' mechanism to create such hot spots in the inner disc and (probably) in the hotter 'thermal boundary layer', which creates oscillations highly coherent and sinusoidal with all the characteristics of the observed DNOs.

We believe the third kind of oscillations, whit.11 is transient and has a low frequency, is more related to the so-called Quasiperiodic Oscillations (QPOs).

The present results, however, cannot explain the flickering observed in the inner region of cool discs in CV systems, though it is believed to originate from an inner turbulent disc (e.g. Bruch 1992).

5 Conclusions

We have followed the non-linear growth of non-axisymmetric instability in geometrically thin Keplerian discs. The instability cicvc1oim in the inner disc when the inner boundary is rigid (corresponding here to the surface of an accreting compact star) and when the disc is neither too hot (say with a Mach number M > 15) neither too viscous. All the modes of the instability have a high Q values and a period of rotation of the order of the Keplerian period at the inner edge of the disc. The high order modes have growth rate larger than the low order modes. in CV discs the viscosity parameter is expected to be $\alpha \approx$ I, 10-1, however in the inner region (boundary layer) the viscosity drop by several orders of magnitude, and there $\alpha \approx 10^{-3}$ (e.g. Regev 19S3). Here we consider both cases. When assuming a high viscosity ($\alpha =$ 0.1) the higher modes are first to be damped and saturate at moderate values: the energy is contained in the low order modes which dominate the flow. When the viscosity is low ($\alpha =$ 0.001), the high order modes dominate the flow, while the low order modes do not grow (tile energy is contained in the higher modes). When the order m and the amplitude a of the unstable mode are high enough, the flow undergoes a (subcritical) transition to turbulence. The turbulence is confined in the inner region of the disc, inside the 'resonant cavity', where it sustains itself due to the over reflection of waves. Some of the low 01'(1('1' 1110(1('s (e.g. m=5, quite amazingly similar to the results of Dubrulle 1991 in a 3D Couette flow) are dominant during transient phases of the turbulent flow, but eventually the m=1 mode dominates the [low (this is a common situation in 2D turbulence, since the m=1 mode corresponds to the largest Scale available for tile development of the turbulence with an inverse cascade of energy). The turbulence obtained in this work cannot account for angular momentum transport in the disc. neither can the outward propagating waves (e.g. Kaisig 1989a, 1989b). Waves which can transfer angular momentum are inward propagating waves (Spruit 19S9), excited in tile outer disc (e. g by tidal forces, see Paper I). It is now believed that a hydromagnetic instability (the Velikhov-Chandrasekhar instability) is responsible for the transport of angular momentum in the disc (Halbus & Hawley 1991). However, tile present results provide a new mechanism to explain the appearance of short period oscillations observed in the inner disc of cataclysmic Variables and other related systems. We identified in the turbulent inner disc highly coherent and sinusoidal oscillation, with a roughly Keplerian period, together with its first harmonic, that easily explains the appearance of DNOs in CVs. A less coherent oscillation with a longer period is also observed, clue to eccentric oscillations of the disc. This latter oscillations is more characteristic of the QPOs observed in these systems.

The present work has an additional direct implication for two-dimensional compressible transonic shear flow's like the one studied by Tomasini et al. (1996). In their numerical simulations Tomasini et al. show that a centrifugal instability dominates the flow without transition to turbulence. However, these authors remark that the absence of turbulence is probably clue to the low Reynolds number and low resolution. The centrifugal instability is related to a strong shear in the flow, and it is not known whether some link exists between the centrifugal instability and the Papaloizou-Pringle instability. However, if a relation exists between the two, then there are good reasons to think that the centrifugal instability might also leads to a subcritical transition to turbulence in tile two-dimensional compressible rotating shear layer flow studied by Tomasini et al. (1996), provided the amplitude and the order of tile unstable mode are high enough.

A high resolution study of the instability in the inner disc will be carried out in the future. A high resolution spectral code will enable to include the effects of the dynamical boundary layer on the solution. It is possible that the very large shear in the boundary layer is enough to sustain turbulence in the flow, without the need for a resonant cavity and non-axisymmetric unstable modes.

Acknowledgments

I am thankful to Bérengère Dubrulle and James Cho for discussions on turbulence. 1 thank Peter Goldreich for comments on the results and Giora Shaviv for discussing some numerical issues related to turbulence. André van Teeseling, Chris Mauche and James Cho have provided me with reprints of their papers. The numerical simulations were performed on a SPARC station 20. I am grateful to David Meier and David Murphy for providing additional running time on their SPARC station. This work was started while the author held a National Research Council - (NASA Jet Propulsion laboratory) Research Associateship. This research was carried out at the Jet ~'repulsion Laboratory, California institute of Technology, under contract to the National Aeronautics and Space Administration.

References

1. Balbus, S. A., & Hawley, J. F. 1991, ApJ, 376, 214
2. Balbus, S. A., Hawley, J. F., & Stone, J. M. 1996, ApJ, 467, 76
3. Bath, G. T. 1973, Nature Phys. Sci., 246, 84
4. Bayly, B. J., Orszag, S. A., & Herbert, '1'. 1988, Ann. Rev. Fluid Mech., 20, 359
5. Blats, O. M. 1987, MNRAS, 227, 975
6. Blaes, O. M., & Glatzel W. 1986, MNRAS, 220, 253
7. Blaes, O. M., & Hawley J. F. 1988, ApJ, 326, 277
S. Bruch, A. 1992, A & A, 266, 237
9. Canuto, C., Hussaini, M. Y., Quarteroni, A. & Zang, T. A. 1988, Spectral Methods in Fluid Dynamics (New York: Springer Verlag)
10. Chandrasekhar, S. 1961, Hydrodynamic and Hydromagnetic Stability, (oxford [University Press)
11. Cho, J. Y. K., & Polvani, L. M. 1996a, Phys. Fluids, 8 (6), 1531
12. Cho, J. Y. K., & Polvani, L. M. 1996b, Science, 273, 335
13. ('010s, D. 1965, J. Fluid Mech., 21, 385

14. Cushman-Roisin, B. 1994, Introduction to Geophysical Fluid Dynamits. (Prentice-Hall, New Jersey)

15. Daviaud, F., Hegseth, J., & Bergé, P. 1992, Phys. Rev. Let., 69 (17), 2511

16. Dauchot, 0., & Daviaud, F. 1994, Europhys. Lett., 28, 225

17. Dauchot, O., & Daviaud, F. 1995a, Phys. Fluids, 7 (2), 335

18. Dauchot, O., & Daviaud, F. 1995b, Phys.Fluids, 7 (5), 901

19. Don, W. S., & Gottlieb, D. 1990, Comput. Meth. Appl. Mech. Engrg., 80, 39

20. Dubrulle, B. 1991, in P.Sulem & J.-D .Fournier (eds.), Non linear dynamics of structures, (Springer Verlag), 252

21. Dubrulle, B. 1997, private communication

22. Dubrulle, B., & Nazarenko, S. 1994, Europhys. Lett., 27, 129

23. Dubrulle, B., & Valdettaro, L. 1992, A & A, 263, 387

24. Dubrulle, B., & Zahn, J. P. 1991, J. Fluid Mech., 231, 561

25. Drury, L. O'C. 1980, MNRAS, 193, 337

26. Fjørtoft, R. 1950, Geofys. Publ., 17, 52

27. Fujimoto, M. Y. 1987, A & A, *176, 53*

28. Gat, O., & Livio, M. 1992, ApJ, 396, 542

29. Glatzel, W. 1987a, MNRAS, 225, 227

30. Glatzel, W. 1987b, MNRAS, 228, 427

31. Glatzel, W. 1988, MNRAS, 231, 795

32. Glatzel, W. 1989, J.Fluid Mech., 202, 515

33. Godon, P. 1995, MNRAS, 274, 61

34. Godon, P. 1997, ApJ, vol.480, 329 (Paper 1)

35. Goldreich, P., Goodman, J., & Narayan, R. 1986, MNRAS, 221, 339

36. Goldreich, P., & Lynden-Bell, D. 1965, MNRAS, 130, 125

37. Goldreich, 1'., & Narayan, R. 1985, MNRAS, 213, 7

38. Goodman, J., Narayan, R., & Goldreich, P. 1987, MNRAS, 225, 695

39. Gottlieb, D., & Orszag, S.A. 1977, Numerical Analysis of Spectral Methods: Theory and Applications (NSF-CBMS Monograph 26; Philadelphia: SIAM)

40. Hamilton, J. M., & Abernathy, F. H. 1994, J. Fluid Mech., 264, 185

41. Hanawa, T. 19S6, MNRAS, 223, 859

42. Hanawa, T. 1987a, A & A, 179, 383

43. Hanawa, T. 1987b, A & A, 185, 160

44. Hawley, J. II'. 1987, MNRAS, 225, 677

45. Hawley, J. F. 1991, ApJ, 381, 496

46. Hegseth, J. J. 1996, Phys. Rev. E, 54 (5), 4915

47. Hujeirat, A. 1995, A & A, 295, 249

4S. Jaroszyński, M. 19SS, Acts Astron., 3S, 2S9

49. Jones, W. I,. 1968, J. Fluid Mech., 34, 609

50. Kaisig, M. 1989, A & A, 218, 89

51. Kaisig, M. 19S9, A & A, 21S, 102

52. Kley, W. 1991, A & A, 247, 95

53. Landau, L. D., & Lifshitz, E. M. 1987, Fluid Mechanics, Course of Theoretical Physics, vol.6 (Pergamon Press)

54. Lerner, J., & Knobloch, E. 1988, J. Fluid Mech., 1S9, 117

55. Lighthill, M. J. 1978, Waves in Fluids, Cambridge University Press

56. Mason, K. O., Middleditch, J., Nelson, J. E. & White, N. E. 1980, Nature, 287, 516

57. Mauche, C. W. 1996, in IAU Colloquium 163 - Accretion Pheonomenon and related outflows, Eds. D. Wickramasinghe, L. Ferrario, & G. Bicknell (San Fransisco: ASP)

58. Mauche, C. W., & Robinson, E. L. 1997, in 13th North American Workshop on Cataclysmic Variables, in press

59. Narayan, R., & Goodman, J. 1989, in Meyer et al. (eds.), Theory of Accretion Disks, (Kluwer Academic Publishers), 231

60. Narayan, R., Goldreich, P., & Goodman, J. 1987, MNRAS, 228, 1

61. Narayan, R., & Popham, R. 1989, ApJ, 346, L25

62. Orszag, S. A., & Kells, L. C. 1980, J. Fluid Mech., 96, 159

63. Papaloizou, J. C. B., & Pringle, J. E. 1984, MNRAS, 208, 721

64. Papaloizou, J. C. B., & Pringle, J. E. 1985, MNRAS, 213, 799

65. Papaloizou, J. C. B., & Pringle, J. E. 1987, MNRAS, 225, 267

66. Patterson, J. 1979, ApJ, 234, 978

67. Patterson, J. 1981, ApJS, 45, 517

68. Pedlosky, J. 1987, Geophysical Fluid Dynamics, 2nd ed. (Springer Verlag, New York)

69. Popham, R, & Narayan, R. 1991, ApJ, 370, 604

70. Rayleigh, Lord 1916, Proc. Roy. Sot. London A 93, 148

71. Regev, O. 1983, A & A, 126, 146

72. Różyczka, M., & Spruit, H. C. 1993, ApJ, 417, 677

73. Savonije, G. J., & Heemskerk, M. H. M. 1990, A & A, 240, 191

74. Sadeh, D., Byram, E. T., Chubb, T. A., Friedman, H., Hedler, R. L., Meekins, J. F., Wood, K. S., & Yentis, D. J. 1982, ApJ, 257, 214

75. Schoelkopf, R. J., & Kelley, R. L. 1991. ApJ, 375, 696

76. Sekiya, M., & Shoken, M. N]. 1988. MNRAS, 234, 107

77. Shakura, N. I., & Sunyaev, R. A. 1973. A & A, 24, 337.

78. She, Z.S., Jackson, E., & Orszag, . SA. 1 991, Proceedings of the Royal Society of London, Series A: Mathematical and Physical Sciences, vol. 434 (1s90), 101.

79. Spruit, H.C. 1989, in F. Meyer et al. (eds.), Theory of Accretion Disks, 325, Kluwer Academic Publishers

SO. Stewart, J.M. 1975, A & A, 42, 95

81. Stewart, J.M. 1976, A & A, 49, 39

82. Strohmayer, T. E., Zhang, W., Swank, J. H., Smale, A., Titarchuk, L. Day, C., & Lee, U. 1996, ApJ, 469, L9

83. Sung, C.-H. 1974, A & A, 33, 99

84. Teeseling, van A. 1997, A & A, in press

S5. Tomasini, NJ., Dolez, N., & Léorat, J. 1996, J. Fluid Mech., 306, 59

86. Voigt, R.G. , Gottlieb, D., & Hussaini, M.Y. 19S4, Spectra] Methods for Partial Differential Equations (Philadelphia: SIAM-CBMS)

87. Warner, 11.1986, Ap& SS, 118, 271

88. Zahn, J. P. 1990, in Bertout, C., Collin-Souffrin, S., Lasota, J. P., & Tran Than, Van J., (eds.), Structure and emission properties of accretion discs, Edition Frontiїes

Figures caption

Figure 1.
A grayscale of the density is shown. An m= 16 mode has grown in the inner disc. Waves propagate outwards from the corotation radius into the outer region of the disc.

Figure 2.
A grayscale of the density is shown. An m=19 mode has grown in the inner disc, from where waves propagate outwards into the outer region of the disc.

Figure 3.
A grayscale of the density is shown in the inner disc in which all the modes have grown unstable. The flow is turbulent in the inner disc, from where

waves propagate outwards into the outer disc. Here the modes 5 and 19 are stronger than the other modes.

Figure 4.
The total kinetic energy in the inner disc $E_k = \frac{1}{2}\rho v_\phi^2 + \frac{1}{2}\rho v_r^2$ is drawn (in arbitrary units) as a function of time (in units of Keplerian rotation period at the inner edge of the disc $2\pi/\Omega_K(R_{in})$). The Keplerian 'background' velocity has been substracted to v_ϕ. The energy has been integrated radially over the inner turbulent region, and azimuthally over 2π. Around t = 400 the energy reaches a plateau when the unstable m=19 mode starts to saturate. At this time the mode has stopped to grow exponentially, but continues to grow linearly. The energy undergoes an additional growth around $t \approx$ 650 – 700 when the flow becomes turbulent. The flow stays in the turbulent state for t >700 till $t \approx$ 1200.

Figure 5.
The total kinetic energy spectrum is shown, integrated in time and in the radial direction over the inner turbulent region. The spectral decomposition has been carried out in the azimuthal direction. The spectrum is S11OW11 before the transition to turbulence, while the m=19 mode is dominant.

Figure 6
Same as figure 5, but the spectrum is shown after the transition to turbulence. During most of that time a few modes are stronger than the others, these modes are the m=1, 5, and 19. The slope of the spectrum at the onset of the turbulence initially reaches ≈ -1, and increases slightly with time(≈ -1.5). At $t \approx 850$ the m=1 mode increases and becomes dominant for the rest of the run (i.e. till $t \approx 1200$).

Figure 7.
Some individual modes are drawn as a function of time. The amplitude S_m of each mode m is drawn in units of S_0. The mode m=19 (full line), which eventually leads to turbulence, is shown together with 3 other modes: m=5 (dash), m=10 (dot-dash) and m=15 (dot).

Figure 8.
The energy dissipated in the inner disc is shown (in arbitrary units) as a function of time (local Keplerian orbit at the inner edge of the disc), immediately after the onset of the turbulence around t=770. The upper graph shows the energy dissipated in the inner disc for $0 \leq \phi \leq 2\pi$ ($\Phi_{2\pi}$), while the

lower graph shows the energy dissipated for $0 \leq \phi \leq \pi$ ($@_T$), equivalent to the inner disc eclipsed by the central star.

Figure 9.
This figure is the same as figure S but for $t \approx 1100$.

TABLE 1

EFFECTS OF THE VISCOSITY ON THE $m = 2$ MODE IN A COOL DISC

α	ω_2/Ω_{in}	Ω_{in}/f
0.1	4.24×10^{-3}	1.24
0.125	5.18×10^{-3}	1.24
0.15	6.28×10^{-3}	1.23
0.2	8.06×10^{-3}	1.17
0.3	1.25×10^{-2}	1.14

The α viscosity parameter is given in the first column. The growth rate of the mode is given in column 2 in units of the rotation rate at the inner radius $\Omega_{in} = \Omega_K(r = R_{in})$. The rotation period of the mode $(p = 2\pi/f)$ is given in the last column in unit of the local Keplerian rotation period of the inner radius $(2\pi/\Omega_{in})$.

TABLE 2

GROWTH RATES AND MODES FOR DIFFERENT VALUES OF THE VISCOSITY

α	ω_2/Ω_{in}	m
0.1	4.24×10^{-3}	2*
0.1	8.83×10^{-3}	4
0.1	1.25×10^{-2}	6
0.1	1.54×10^{-2}	8
0.1	1.82×10^{-2}	10
0.1	2.19×10^{-2}	12
0.01	8.86×10^{-3}	9*
0.001	3.89×10^{-2}	19*
0.001	6.45×10^{-2}	24*

The α viscosity parameter is given in the first column. The growth rate of the mode is given in column 2 in units of the rotation rate at the inner radius $\Omega_{in} = \Omega_K(r = R_{in})$. The order of the mode m is given in the last column. An asterix denotes that the mode was the dominant one in the run.

TABLE 3

EFFECTS OF THE VISCOSITY ON THE ORDER OF THE DOMINANT MODE IN A COOL DISC

α	m	$N \times M$
0.1	2	64X32
0.01	8-5	256X32
0.001	>20	256X64

The α viscosity parameter is given in the first column. The order of the dominant modes is given in column 2. The resolution is given in column 3. N is the number of points in the radial direction and M is the number of points in the angular direction.

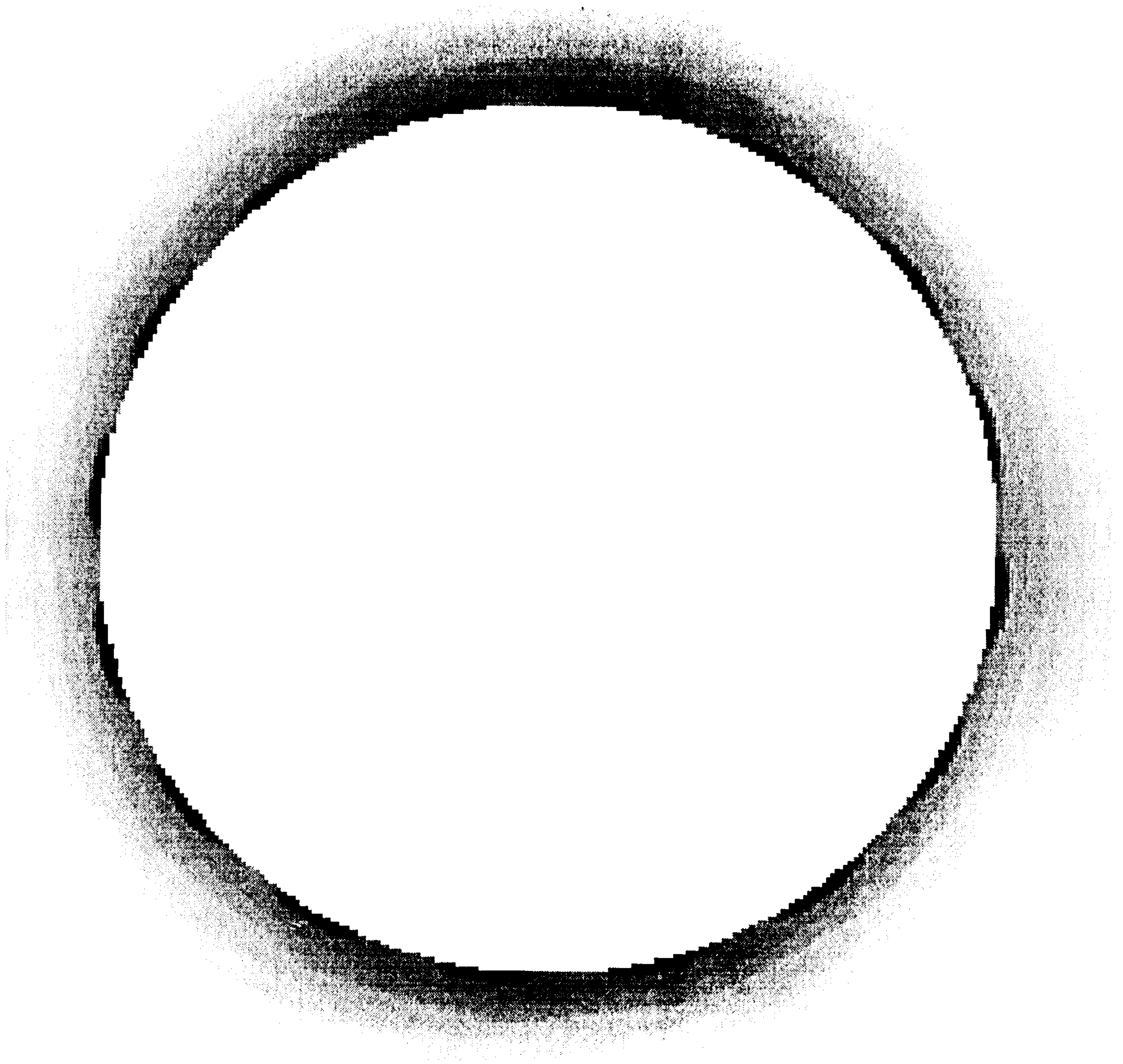

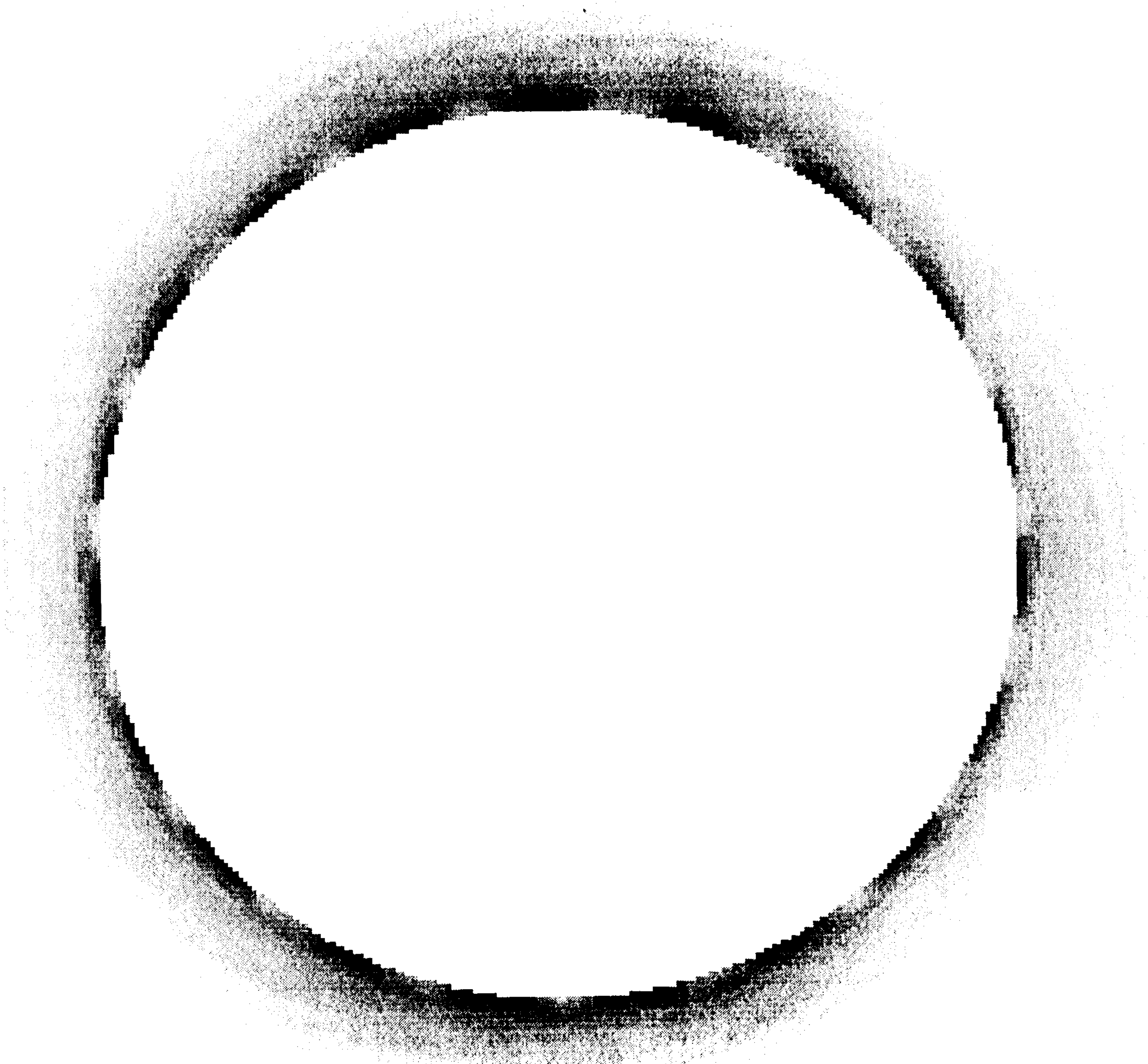

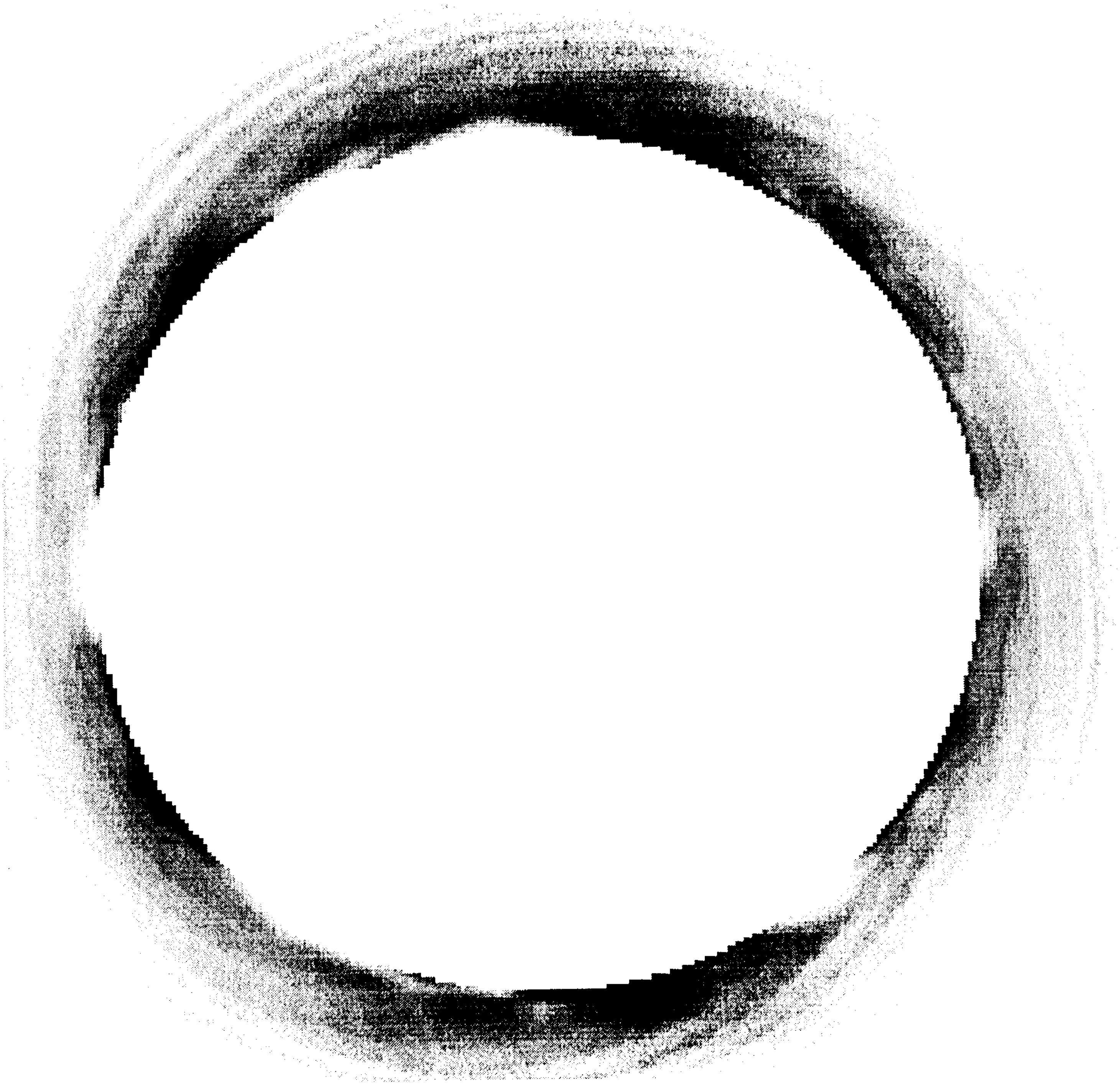

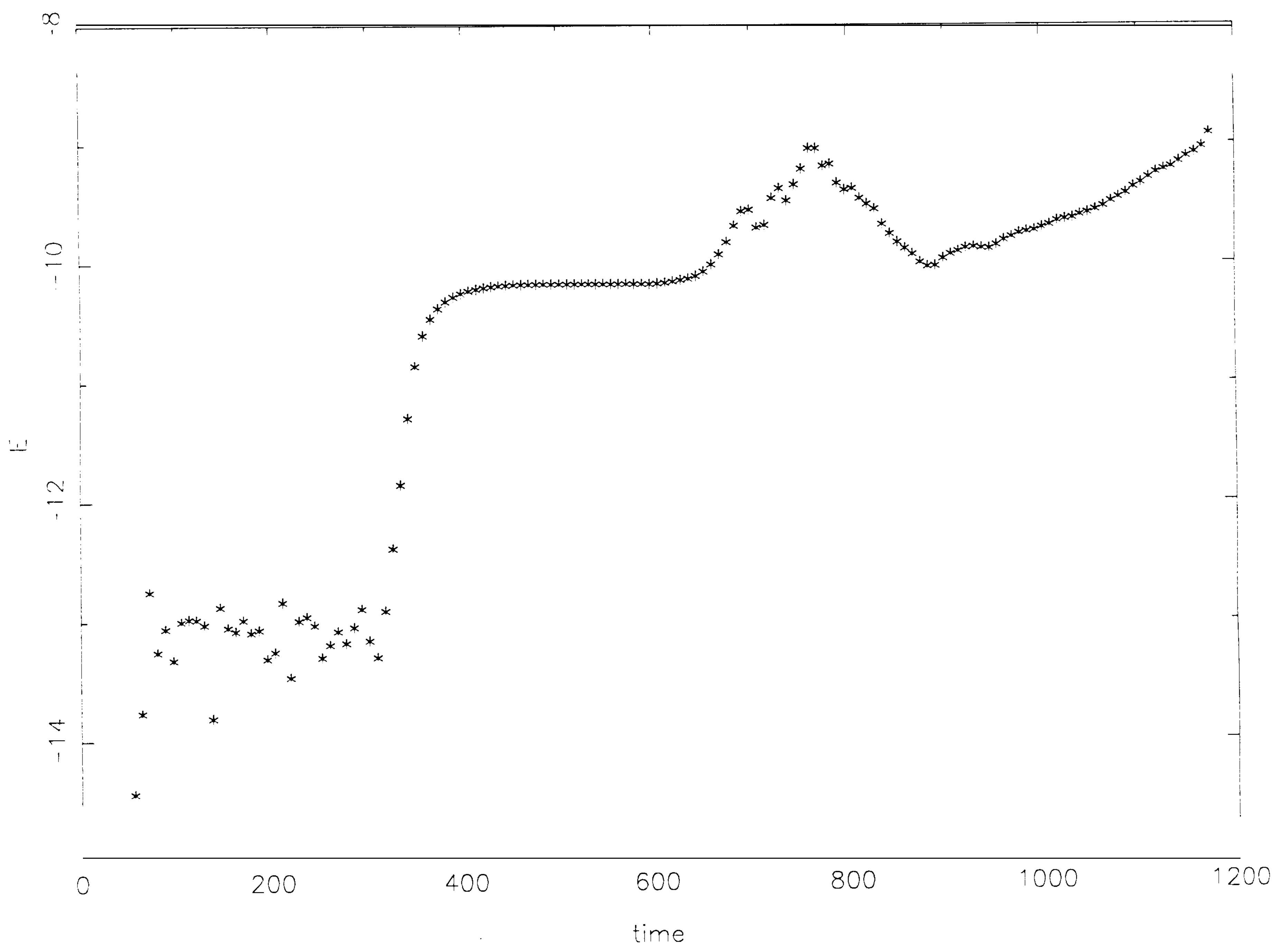
-8
-10
-12
-14
E
0
200
400
600
800
1000
1200
time

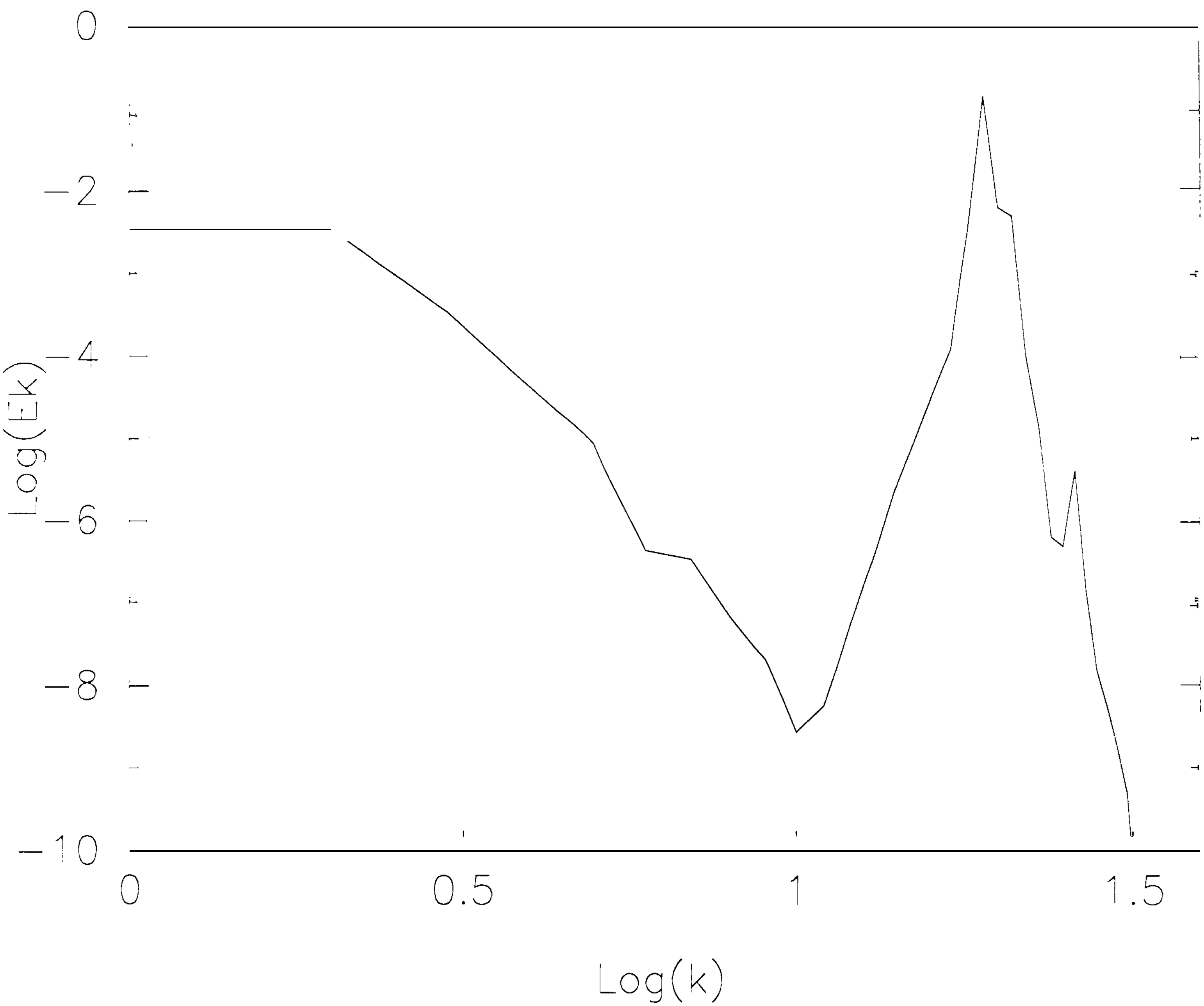
0
−2
−4
−6
−8
−10
Log(Ek)
0
0.5
1
1.5
Log(k)

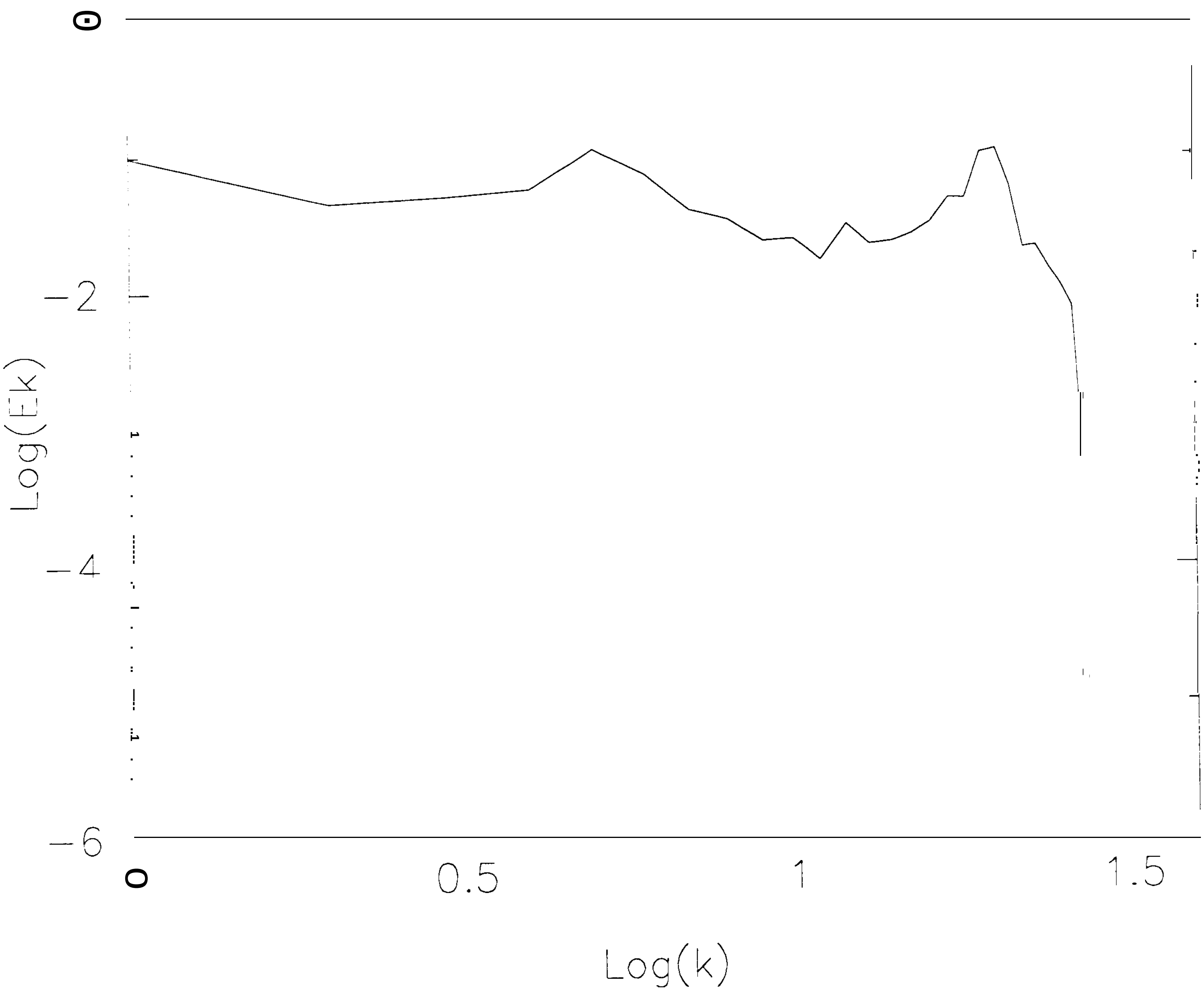
0
−2
−4
−6
Log(Ek)
0
0.5
1
1.5
Log(k)

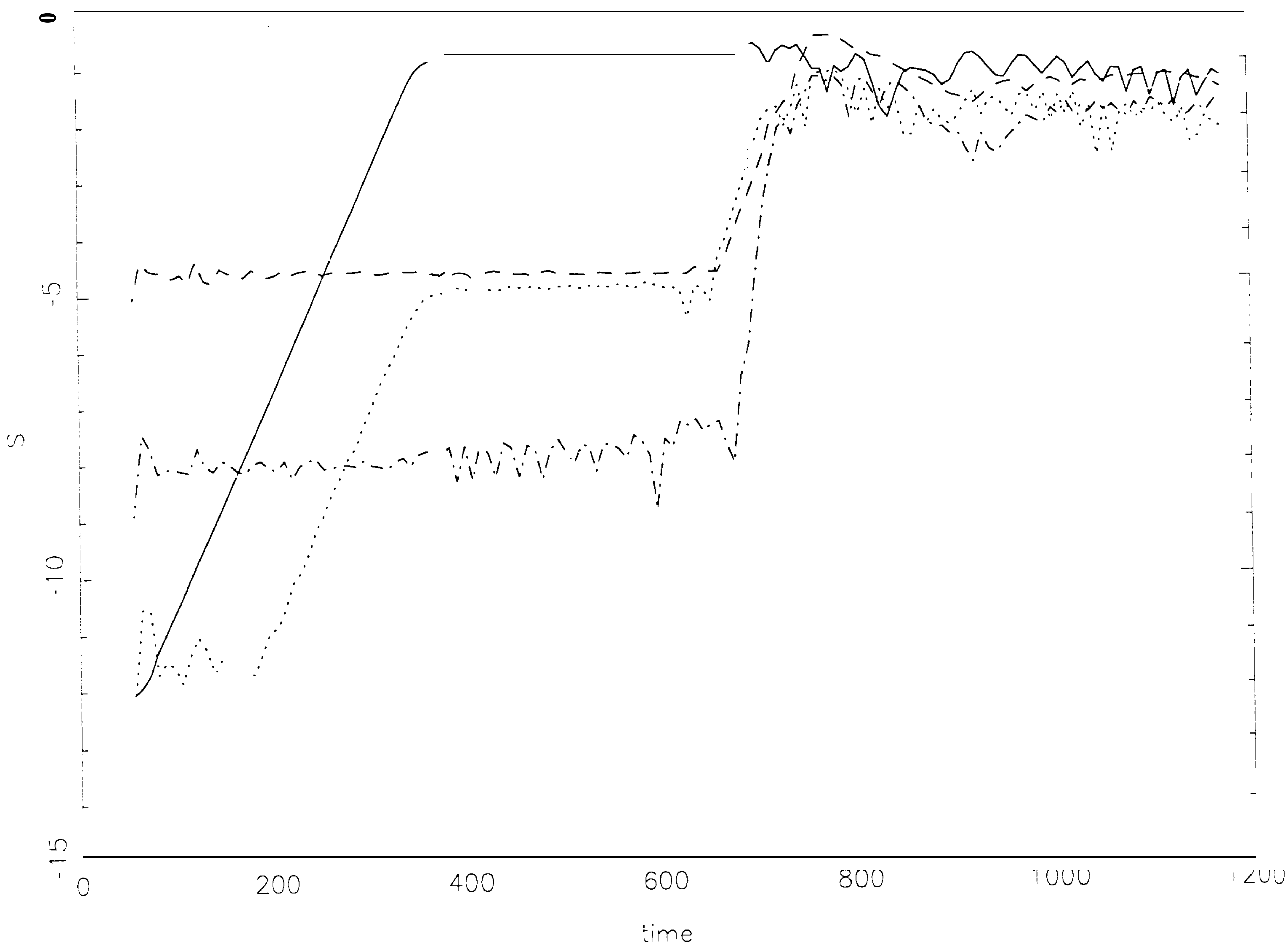

0
-5
-10
-15
S
0
200
400
600
800
1000
1200
time

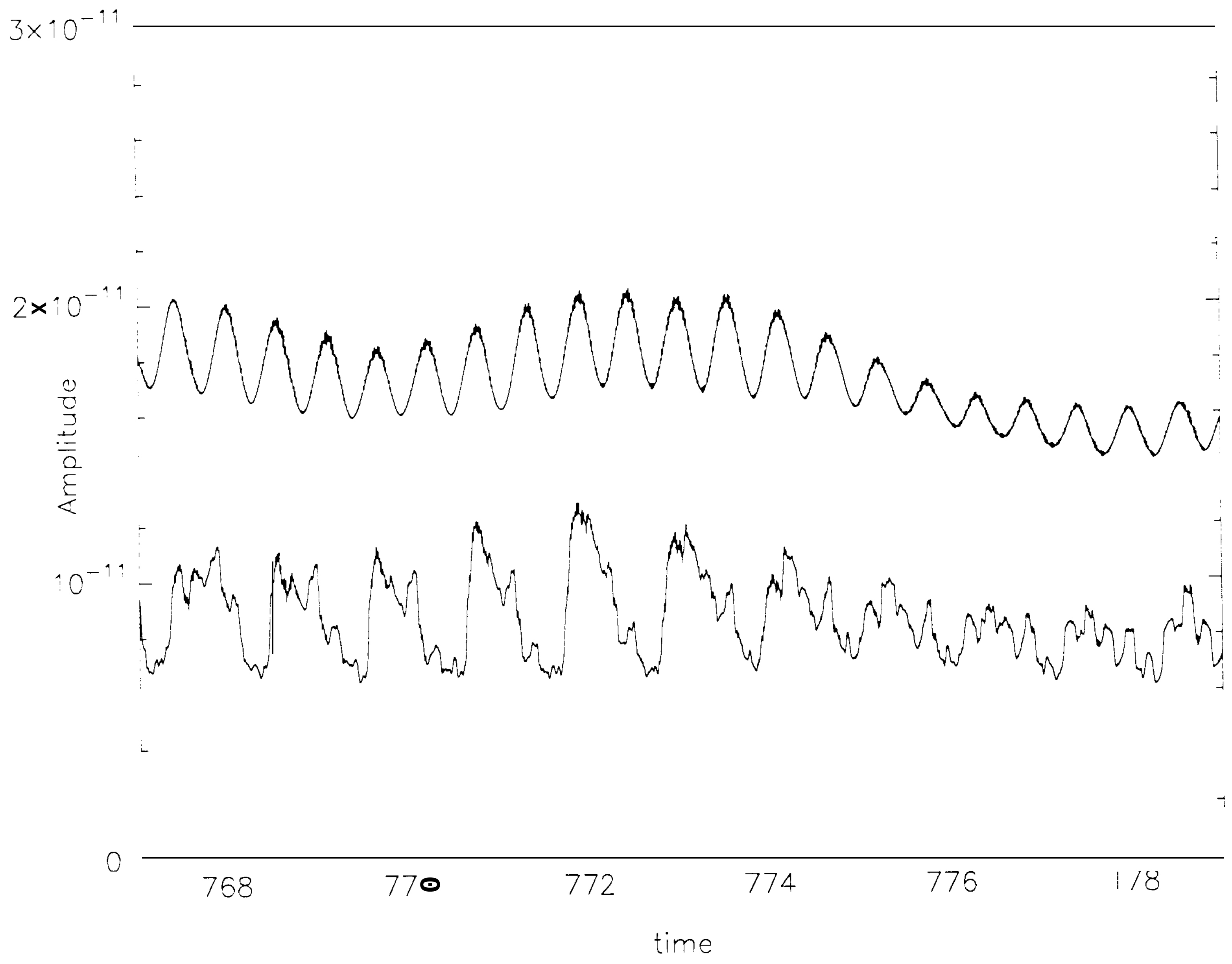

3×10^{-11}
2×10^{-11}
Amplitude
10^{-11}
0
768
770
772
774
776
778
time

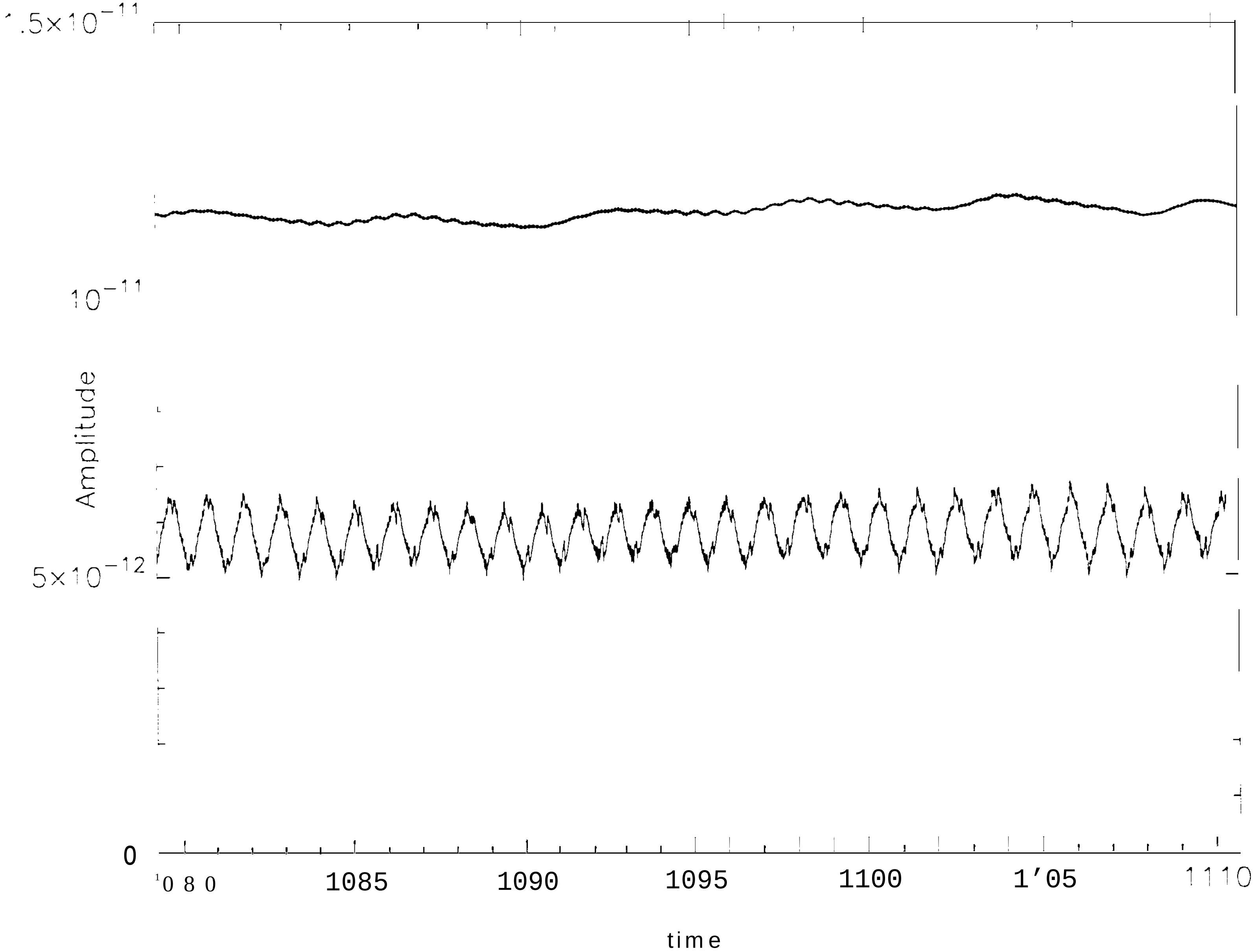

1.5×10⁻¹¹
10⁻¹¹
5×10⁻¹²
0
Amplitude
1080
1085
1090
1095
1100
1105
1110
time